Comparison of Deep Foundation Systems using 3D Finite Element Analysis Employing Different Modeling Techniques

F. Tschuchnigg & H.F. Schweiger
[1]*Institute for Soil Mechanics and Foundation Engineering, Graz University of Technology, Graz, Austria*
E-mail: franz.tschuchnigg@tugraz.at

ABSTRACT: Finite element analyses for the deep foundation of the Donau City Towers in Vienna are discussed in this paper. The towers are located very close to each other, thus interaction of the two towers has to be taken into account for the design of the foundation system. The objective of the analysis was twofold, namely to calculate maximum and differential settlements to be expected and optimisation of the layout of the foundation elements. In addition to the foundation concept actually constructed alternative solutions have been studied in a numerical study and the results of this study are presented in this paper. Different techniques for modelling the foundation elements in the numerical model, namely a standard approach using volume elements and the embedded pile concept, are investigated. The latter approach is discussed is some detail before the case study is presented.

1. INTRODUCTION

Deep foundations such as pile foundations or piled raft foundations require in general three-dimensional numerical analyses. The problem when modelling deep foundations in 2D is that the geometry and the layout of the foundation elements do not allow a plane strain representation and one has to modify either the dimensions or the stiffness of the deep foundation elements, e.g. Desai et al. (1974) or Prakosa & Kulhawy (2001). A combination of both approaches is the best choice for normal circumstances. But once the spacing between the piles is large the equivalent stiffness method should be adopted, otherwise, relatively small pile dimensions have to be used, leading to a different behaviour of the piles.

A number of authors investigated the behaviour of deep foundations by means of FEM. Chow & Teh (1991) studied the behaviour of vertically-loaded pile groups in nonhomogeneous soil. Liu & Novak (1991) studied the pile-soil interaction of a raft supported by a single pile by means of finite and infinite elements. Arslan et al. (1994) conducted 3D finite element analysis of piled raft foundations using an elasto-plastic constitutive model. Reul (2004) demonstrated with numerical studies the influence of pile-pile and pile-raft interaction within a piled raft foundation. Recently, Wehnert et al. (2010) presented back-analyses of three pile load tests by means of 2D and 3D calculations and finally a settlement analysis of a piled raft foundation supported by more than 500 large diameter bored piles. They stated that for the boundary value problem considered, neither a 2D cross section nor a simplified model of a specific part of the deep foundation would have been adequate to predict the differential settlements.

One of the key aspects in numerical modelling of this type of problems is an appropriate model to take into account the interaction between piles and surrounding soil. This interaction behaviour is different depending on the type of foundation, e.g. piled raft foundations as compared to a standard pile foundation, and strictly speaking also depends on type of piles and the construction method. In the FE-Code Plaxis 3D Foundation (Brinkgreve & Swolfs, 2007), which is used for all analyses discussed here, soil-structure interaction is taken into account by means of interface elements when the foundation elements are modelled with volume elements. These interface element have a reduced strength with respect to the strength of the surrounding soil by introducing a strength reduction factor R_{inter} (Eq. 1, 2 and 3).

$$c'_i = R_{inter} \cdot c' \tag{1}$$

$$\tan\varphi'_i = R_{inter} \cdot \tan\varphi' \leq \tan\varphi'_{soil} \tag{2}$$

$$\psi_i = 0° \; for \; R_{inter} < 1.0, \; otherwise \; \psi_i = \psi \tag{3}$$

Another option for modelling piles is the concept of a so-called embedded pile element. This special element, also available in the Plaxis element library, consists of a beam element which can be placed in arbitrary direction in the subsoil, embedded interface elements to model the interaction of the structure and the surrounding soil and embedded non-linear spring elements at the pile tip to account for base resistance. When the embedded pile option is used additional nodes are automatically generated inside the existing finite elements and the pile-soil interaction behaviour is linked to the relative displacements between the pile nodes and the existing soil nodes (Sadek & Shahrour, 2004).

The big advantage of this concept is that different pile lengths, spacing and orientation can be studied without regenerating the entire finite element mesh. If a large number of piles has to be considered the number of elements in the system is significantly reduced as compared to finite element models with volume piles. In order to assess the applicability of the embedded pile approach for practical problems the behaviour of a piled raft foundation with varying geometry is studied first. The key question inspected in this paper is the mobilisation of the skin friction and the settlement behaviour with respect to different piled raft geometries using a unit cell approach in axisymmetric conditions and 3D analysis using volume elements and embedded pile elements.

2. GEOMETRY AND MATERIAL PARAMETERS FOR BASIC STUDY

In order to compare axisymmetric analysis with 3D analysis employing volume discretisation for the piles and the embedded pile concept a simplified model based on a "unit cell approach" is chosen. Two aspects are addressed, namely the influence of pile spacing and secondly the influence of how the pile is modelled (volume element vs embedded pile).

Figure 1 shows the general layout of the model and Table 1 the dimensions of the different models discussed in the following. Two geometric conditions are considered in these studies, namely piled raft I and piled raft II, which differ in the spacing of the piles, i.e. the dimension of the unit cell. The most important geometrical relation is the ratio between raft width divided by the diameter of the pile. For all studies presented in this paper the same soil, a dense sand, is used and no groundwater table is present.

The soil is modelled with the Hardening Soil model, a double hardening model available in the Plaxis constitutive model library and the input parameters, which can be considered as typical for a dense sand, are summarized in Table 2.

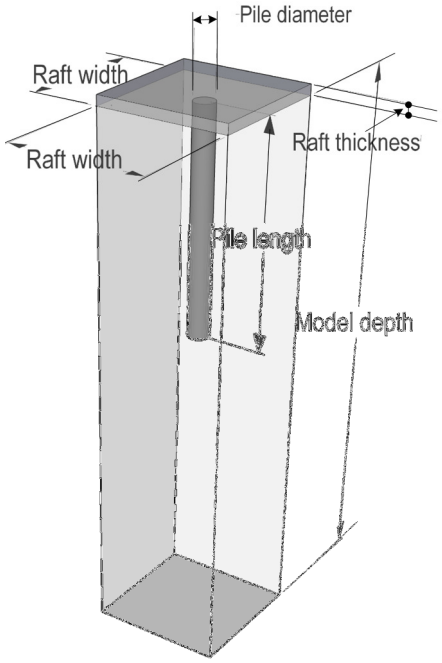

Figure 1 Geometry of simplified piled raft foundation ("unit cell")

Table 1 Dimensions of simplified piled raft foundation

Parameter	Symbol	Piled raft I	Piled raft II
Pile diameter	D_{pile}	0.8 m	0.8 m
Pile length	L_{pile}	15.0 m	15.0 m
Raft width	B_{raft}	2.0 m	5.0 m
Raft thickness	t_{raft}	0.5 m	0.5 m
Model depth	H_{model}	40.0 m	40.0 m
B_{raft}/D_{pile}	-	2.5	6.25

Table 2 Material parameters for dense sand

Parameter	Symbol	Dense sand	Unit
Material Model	-	Hardening Soil	-
Material type	-	Drained	-
Unsaturated weight	γ_{unsat}	21.0	kN/m^3
Stiffness	E_{50}^{ref}	60 000	kN/m^2
	E_{oed}^{ref}	60 000	kN/m^2
	E_{ur}^{ref}	180 000	kN/m^2
Power index	m	0.55	-
Poisson's ratio	ν_{ur}	0.2	-
Friction angle	ψ	8.0	°
Cohesion	c'	0.0	kN/m^2
Failure ration	R_f	0.9	-

3. COMPARISON OF DIFFERENT MODELS

3.1 Axisymmetric model

First results of axisymmetric models are discussed. The model for geometry piled raft I consists of 460 and the model for geometry piled raft II of 750, 15 noded elements. The pile soil interaction is modelled by means of interface elements and at the top of the raft a constant distributed load is applied. Figure 2 shows the mobilised skin friction of piled raft I for different load levels and in addition the distribution of shear stresses for a single pile subjected to a point load of 2000 kN. Figure 3 shows the influence of the dilatancy angle on the skin resistance for geometry piled raft II.

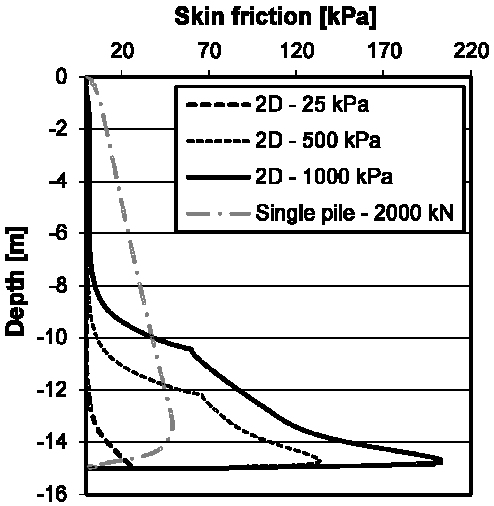

Figure 2 Skin friction distribution for geometry piled raft I and a single pile

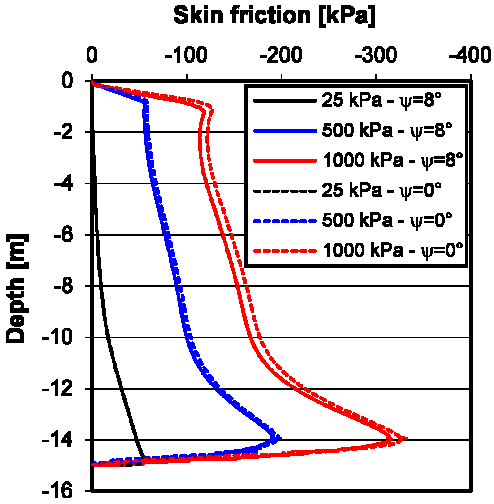

Figure 3 Skin friction distribution for geometry piled raft II

One can see that for piled raft I, piled raft II and a single pile the skin friction is mobilised in a different form. For a single pile the distribution of the skin friction increases with depth, due to the fact that the shear stress is related to the effective normal stress σ'_n along a pile. Equation 4 defines the maximum acceptable shear stress along an interface.

$$\tau_{max} = R_{inter} \cdot \sigma'_n \cdot \tan\varphi' + R_{inter} \cdot c'_{soil} \quad (4)$$

For geometry piled raft I, where the spacing between the piles is relatively small, almost no skin friction is mobilised at the top of the pile. For piled raft geometry II the mobilisation of shaft resistance is strongly influenced by the pile-raft interaction. As a consequence of the load transfer from the raft to the soil the stress state in the soil and as a result of that also the maximum skin friction τ_{max} increases.

In order to check the influence the effect of the R_{inter} value a variation of interface strength has been performed. It follows from Figure 4 that the influence is significantly less compared to the behaviour of a single pile, which is also depicted in Figure 4.

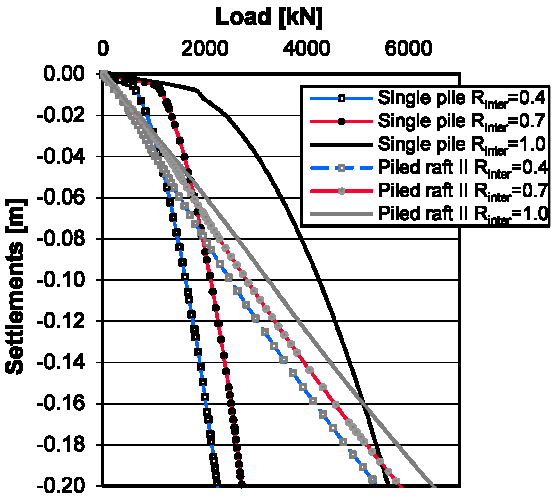

Figure 4 Load-settlement behaviour of single pile versus piled raft foundations

3.2 3D calculations with standard finite element approach

In the standard finite element approach piles are discretized by means of volume elements, which leads to very large finite element models and thus this approach has limits in practical engineering where time and financial restraints often do not allow very complex analyses.

However, to have a reference for the embedded pile model, again the simplified unit cell problem is considered (Figure 1). For piled raft I the model consists of 12 600 and for piled raft II of 22 230, 15 noded wedge elements. It follows from Figure 5 that, as expected, results are in very good agreement with the axisymmetric calculations.

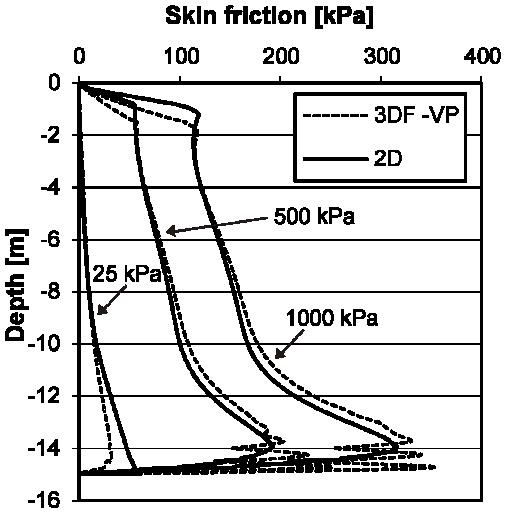

Figure 5 Behaviour of volume piles (VP) for piled raft geometry II

3.3 3D calculations with the embedded pile concept

Although the diameter d, the unit weight γ and the stiffness E are assigned to the embedded beam element, it remains a line element in the finite element model.

The diameter d in the material data set determines an elastic zone in the soil around the beam in order to avoid failure in a soil element which should physically be a pile element (Engin, 2006). A maximum base resistance (F_{max}) is assigned to the non-linear spring elements at the base of an embedded pile. For the definition of the skin resistance three different options are available. The first and simplest one is the linear distribution, where a constant or linear distribution for the ultimate skin resistance is defined. The second option is the so called multilinear distribution where it is possible to define different values for the skin friction in certain depths. This is for example necessary when layered soil conditions and therefore different skin resistances are present along the pile. It is important to notice that this definition implies that the bearing capacity of the pile is an input and not a result of the analysis because the maximum skin friction is predefined. The third way to define the skin resistance is the layer dependent option, where the interface behaviour is related to the strength parameters of the soil and the normal stress along the interface. When using the layer dependent option the embedded interface elements behave similar to normal interfaces elements as used for volume piles (Eq. 4) and therefore the input for the layer dependent option is a R_{inter} value for the strength reduction. In addition a limiting value for the skin resistance is defined. Figure 6 illustrates the embedded pile concept.

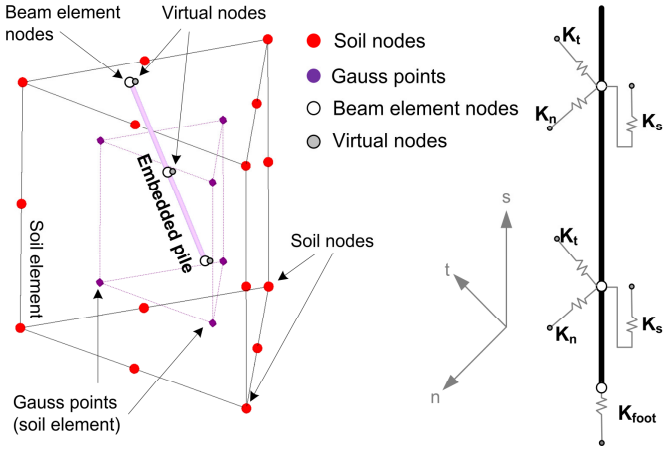

Figure 6 Embedded pile: a) Schematic overview
b) Embedded interface stiffnesses

In this chapter only the results for piled raft geometry II are presented. The model consists of 14 300, 15 noded wedge elements. Table 2 shows the input values for the embedded interfaces for the different calculations performed. It has to be mentioned that an improved version of the embedded pile formulation has been used, which includes an updated definition of embedded interfaces and the elastic region.

The distribution constant is defined with a constant ultimate skin friction of 1110 kN/m. For distribution multilinear, the skin friction profile is defined with the values for the mobilised skin friction obtained in the appropriate axisymmetric model. It is emphasized that the values given in Table 3 are the maximum values which can be reached but as follows from Figure 7, where the mobilised skin friction for a load level of 500 kPa is shown, they do have an influence on the stress distribution also at lower load levels.

Table 3 Parameters for embedded pile interfaces

Skin friction distribution	**Constant [kN/m]**	**Multilinear [kN/m]**
Depth [m]	-	
0.0	1110	0
1.2	1110	315
2.15	1110	290
10.2	1110	430
12.1	1110	553
14.0	1110	804
15.0	1110	0
F_{max} [kN]	8300	8300

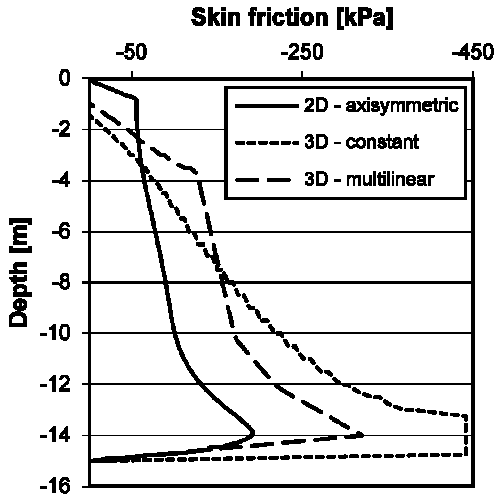

Figure 7 Behaviour of embedded piles (EP) for piled raft geometry II

One can see that the skin friction distribution along an embedded pile, when using the linear or multilinear option to define the profile, is completely different compared to the axisymmetric calculations (which match with the 3D volume piles as shown in the previous section). It seems that an embedded pile always starts to mobilise the skin friction from the bottom and simply "fills up" the predefined skin friction profile. In comparison to the axisymmetric solution the skin friction below failure state is overestimated and the base resistance is underestimated.

Also the change in the stress state at the top of the pile is not taken into account; hence the increase of maximum skin friction due to the raft-soil interaction cannot be modelled with these definitions of ultimate skin friction. If the skin friction at failure should be related to the stress state in the surrounding soil the layer dependent option of the embedded pile concept must be used.

3.4 Conclusion from "unit cell" study

The results from the axisymmetric model are in good agreement with the 3D calculations, when using volume piles. In both models the mobilisation of the skin friction and the global settlement behaviour is almost the same.

With the embedded pile formulation when using the linear or multilinear option the input values for the skin resistance play a significant role. The input values do not only define the final distribution of the shear stresses along a pile, but influence the mobilisation process. From that follows that a change in the stress state of the soil, which could have a big effect on the bearing capacity of piles, cannot be taken into account. Therefore it is not possible to reproduce the results obtained with the standard finite element approach. With the layer dependent definition of the embedded pile the shaft resistance is related to the normal stress on the pile and the change in the stress state in the soil, due to raft-soil and pile-soil interaction is taken into account.

Figure 8 shows the global settlement behaviour of the axisymmetric and 3D models. At a load level of 500kPa the calculation with the constant skin friction distribution computes 5 % less vertical displacements compared to the axisymmetric solution, but as mentioned the skin friction distribution is completely different. When using the more realistic layer dependent skin friction distribution the vertical displacements in this particular case are very similar, but of course a more realistic skin friction distribution is obtained. Thus it can be concluded that the embedded pile option can be used for assessing the settlement behaviour of deep foundations on a global level but further improvements, which are currently investigated, are necessary to obtain a more realistic stress distribution along the pile.

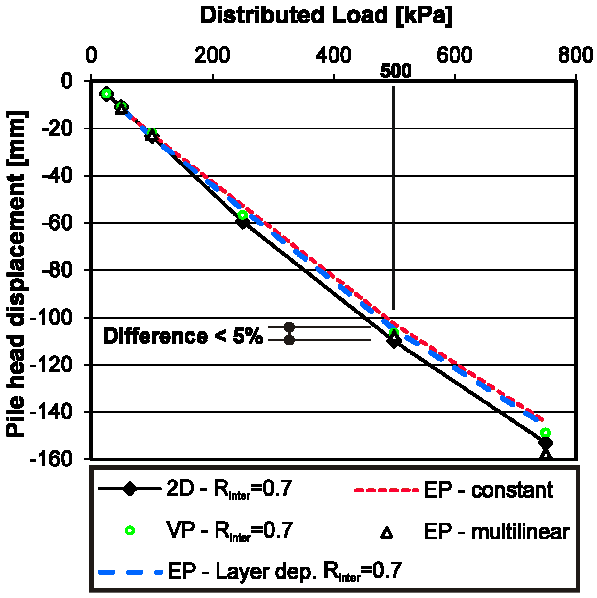

Figure 8 Load-settlement behaviour of different models

4. APPLICATION OF THE EMBEDDED PILE CONCEPT TO A PRACTICAL PROBLEM PROJECT

The project discussed involves two high and slender towers in Vienna. Due to high loads and the existing soil profile a deep foundation is required. In this particular case the deep foundation elements have the form of diaphragm wall barrettes. For these types of foundation systems assessment of settlements and differential settlements are in general the key issues, thus ultimate limit state conditions are not considered here.

4.1 Project overview

Tower I has a total height of about 220 m and tower II of 165 m. Due to the fact that the distance between the two towers is only 24 m it is necessary to take the interaction of the two towers into account. The excavation depth for constructing the base slabs of both towers is about 8.5 m.

4.2 Soil conditions and its numerical modelling

The soil profile defined in the finite element calculations is based on core drillings with depths down to 70.0 m. The first 4 to 5 m consist of deposits, followed by a 6.5 m thick layer of gravel and then alternate layers of either sands or silty clays are present (Martak et al. 2007).

The Hardening Soil Small model (HSS) is used to model the soil behaviour. As a consequence of the small strain stiffness the obtained soil displacements at deeper depths are automatically reduced and a more realistic settlement profile with depth can be obtained (Tschuchnigg & Schweiger 2010).

The HSS model needs, compared to the Hardening Soil Model (Schanz et al. 1999), two additional parameters to describe the stiffness behaviour at small strains. That is the initial shear modulus G_0 and the shear strain level $\gamma_{0.7}$, which represents the shear strain where the secant shear modulus is reduced to 70% of its initial value. Detailed information about the geological conditions and the soil properties are given in Tschuchnigg & Schweiger (2010).

4.3 Calculation procedure

All calculations are carried out as a drained analysis, thus final settlements are presented. The construction process was taken into account by the following phases:

1. Generation of initial stresses
2. Activation of the sheet pile wall for supporting excavation
3. Excavation and groundwater lowering

4. Activation of barrettes (wished in place)
5. Activation of slabs
6. Full loads of tower I and loads from basement floors of tower II
7. Closing of settlement joint - tower I
8. Full loads of tower II
9. Closing of settlement joint - tower II
10. End of ground water lowering

For the generation of the initial stress state it is important to take the overconsolidation of the soil into account. For all soil layers a preconsolidation stress of 600 kPa is defined and the earth pressure coefficient K_0 is assumed to be 0.7 based on local experience. When using the Hardening Soil Small model this has the consequence that the volumetric and deviatoric yield functions are shifted, thus increasing the elastic region.

4.4 Computational models

4.4.1 Deep foundation with diaphragm wall panels

As mentioned before 3D modelling is required for this type of problems. In order to reduce the complexity of the 3D model, in a first step the barrettes of only one tower are modelled in full detail and the foundation system of the other tower is modelled as a homogenized block, meaning that the zones of the subsoil in which panels are installed are defined with smeared properties. With this approach the global settlement behaviour of the entire structure is calculated because the interaction of the towers is taken into account.

However, to validate this modelling assumption an analysis where both foundations are explicitly modelled is presented here. Figure 9 shows a top view of the finite element model for the detailed analysis of both towers and additionally some geometrical information of the project. This model consists of around 137 000 15 noded wedge elements and 317 barrettes are modelled as volume elements.

As the load distribution is highly non-symmetric with respect to the centre of the foundation slab the length of the barrettes has been varied in order to compensate for this and to obtain a symmetric settlement trough. Figure 10 illustrates the final layout of the deep foundation elements and contour lines of vertical displacements. Results of this model will not be discussed in detail here (see Tschuchnigg and Schweiger 2011) but emphasis is put on the different modelling strategies of piled raft foundations.

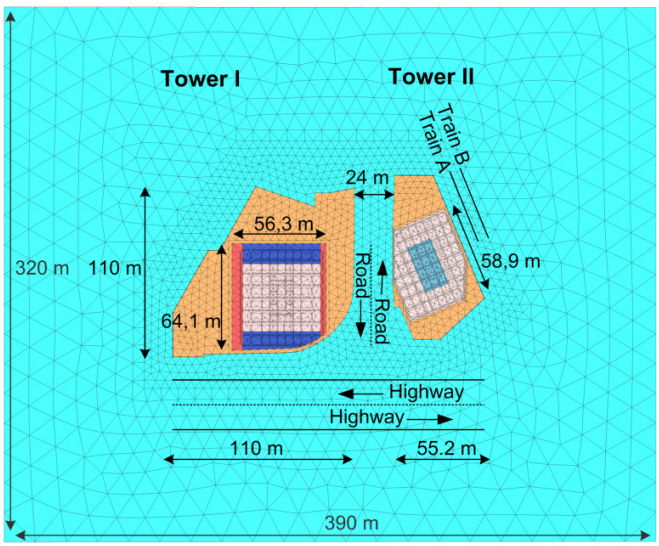

Figure 9 Top view of 3D Finite element model

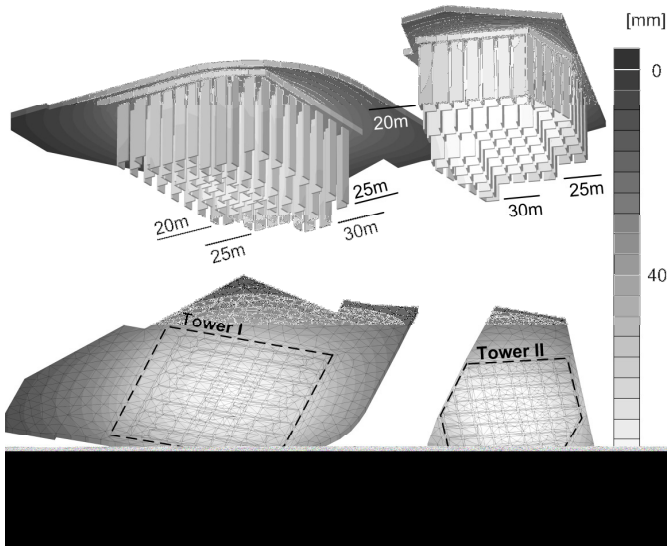

Figure 10 Optimised barrette layout for tower I and tower II

4.4.2 Piled raft foundation with standard finite element approach

The layout shown in Figure 10 is the one actually executed, but unfortunately due to financial constraints only one tower will be built and this is currently under construction. However a numerical study was performed to investigate whether a piled raft foundation with a smaller number of piles would be feasible from a theoretical point of view, notwithstanding the fact that other (contractual or conceptual) issues may have prevented such a solution for this particular project. Different piled raft geometries have been investigated. Figure 11a shows one of the FE models and Figure 11b a bottom view of the analysed piled raft foundation. The vertical model boundaries are free in vertical direction, the model bottom boundary is fixed in all directions and the ground surface is free in all directions.

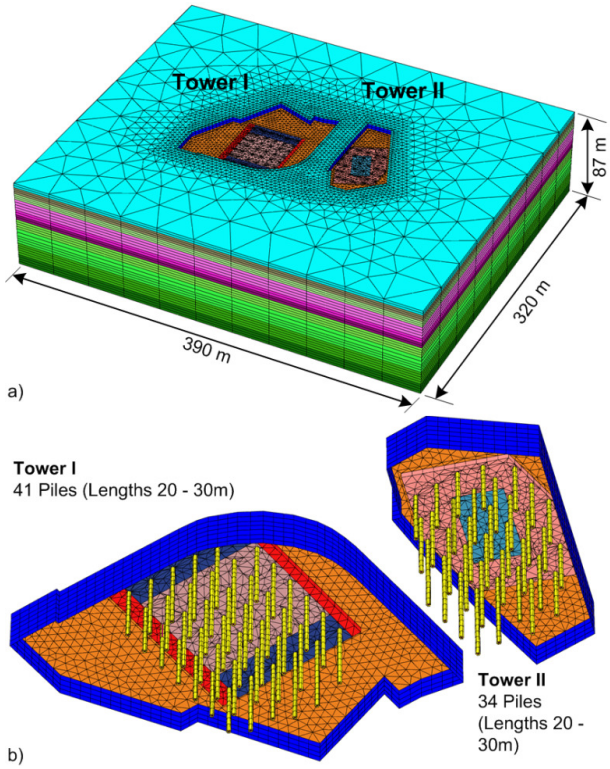

Figure 11 Piled raft foundation: a) Entire 3D model
b) Bottom view of foundation

In this model 75 piles are modelled by means of volume piles (VP). The model consists of 238 272 elements. The number of piles has been chosen by comparison with similar projects presented in the literature and aims firstly to check whether this significant decrease of foundation elements will lead to inacceptable settlements but secondly, and mainly, for comparison with the embedded pile concept. A typical model with embedded piles is shown in Figure 12.

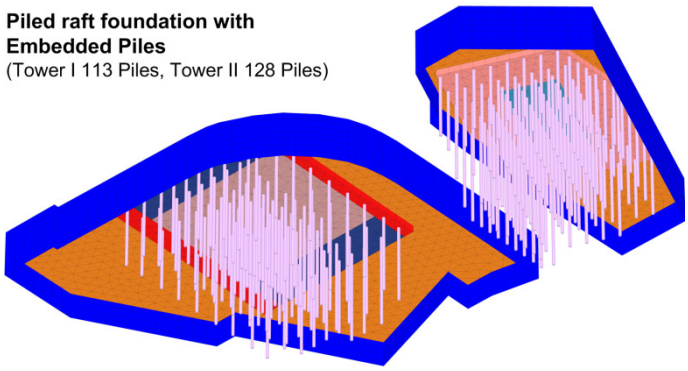

Figure 12 Piled raft foundation with embedded piles

4.4.3 Results

The first layout (Layout 1) studied consists of piles with a radius of 1.5m and a regular spacing of about six times the radius (Figure 11). In this calculation the pile-soil interaction is modelled by means of interface elements with a strength reduction factor R_{inter} of 0.8. The pile length varies between 20 - 30m, similar to the final concept with diaphragm wall panels. This piled raft layout is modelled with both, the embedded pile concept and the standard FE approach. Figure 13 shows that the maximum vertical displacements are almost identical.

However, both the maximum vertical displacements and the differential settlements are not acceptable from a practical point and as a consequence the layout is modified in a way that the spacing of the piles is decreased in the high loaded regions (Layout 2). The length of the piles is again similar to the barrette foundation.

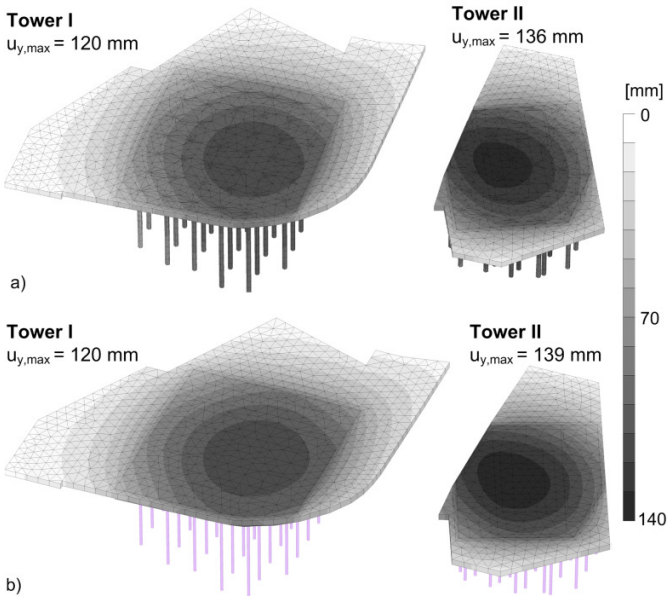

Figure 13 uy of piled raft foundation: a) Volume piles b) Embedded piles

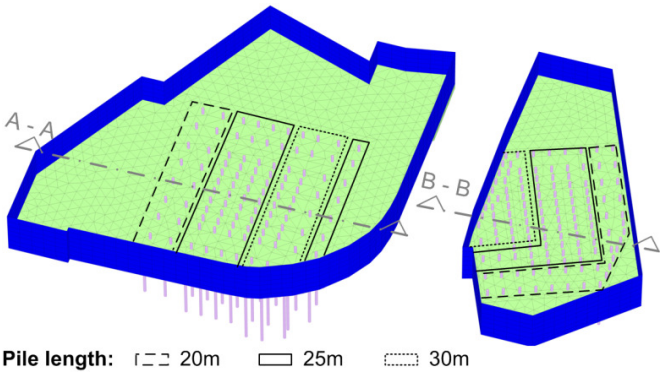

Figure 14 Piled raft foundation with embedded piles

Figure 12 shows a bottom view of the foundation system and Figure 14 a top view, where also the different zones with different pile lengths are highlighted. This piled raft foundation reduces maximum vertical displacements of tower I from 120 mm to 87 mm and settlements of tower II from 139 mm to 88 mm. Also the differential settlements are significantly reduced.

Figure 15 shows the differential settlements of tower I for the different foundation systems. The cross-section A-A is indicated in Figure 14. The barrette foundation concept is compared with piled raft foundation Layout 1, Layout 2 and a shallow foundation. Since Layout 1 is analysed with the standard finite element approach and the embedded pile option both curves are presented.

The shallow foundation yields, as expected, too large vertical and differential settlements. Additionally the maximum vertical displacements are off-centre, which would cause a tilting of the tower. The calculations of Layout 1 have been performed with the standard finite element approach and the embedded pile option. Both calculation models compute almost the same differential settlements, but again unfavourable differential displacements are obtained. Layout 2 with an increased number of piles reduces, compared to Layout 1, both the vertical and differential settlements significantly.

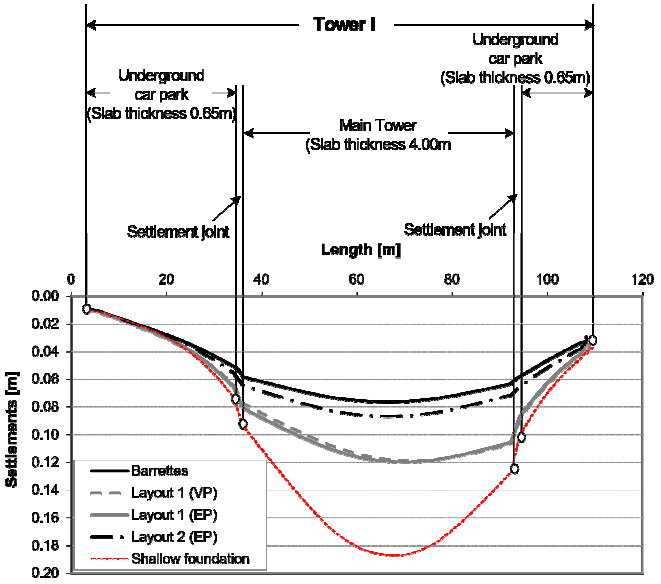

Figure 15 Comparison of settlements (Cross-section A-A)

Figure 16 and Table 4 compare the maximum vertical displacements of the different foundation systems investigated. Additionally the number of deep foundation elements, the total

length and the total volume of barrettes or piles are shown. For the two piled raft foundations the so called α_{PR} factor is also provided. The α_{PR} factor is the ratio between the load carried by the piles (R_{pile}) and the total load (R_{tot}).

$$\alpha_{PR} = \frac{R_{Pile}}{R_{tot}} \tag{5}$$

Table 4 Comparison of foundation systems

Variation	$u_{y,max}$ [cm]	α_{PR} [-]	Nr. El. [-]	Length [10^3 m]	Volume [10^3 m^3]
Shallow Foundation	18.7	-	-	-	-
Barrettes	7.6	-	317	7.84	16.93
Layout 1 (VP)	12.0	0.42	75	1.91	3.37
Layout 1 (EP)	12.0	0.43	75	1.91	3.37
Layout 2 (EP)	8.7	0.8	241	6.12	10.81

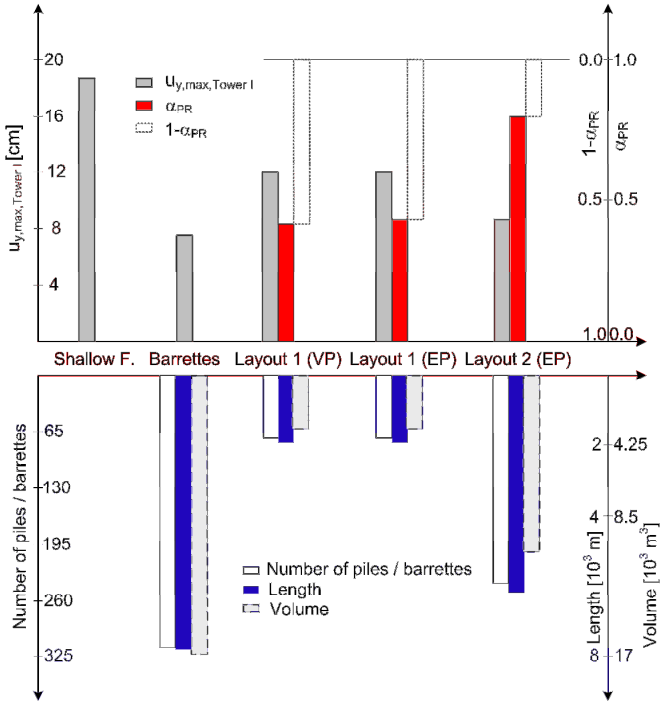

Figure 16 Comparison of foundation systems

5. CONCLUSIONS

In this paper different modelling options of deep foundation elements such as piles and diaphragm wall barrettes have been studied and the results compared. It follows that the embedded pile option can be successfully used for modelling deep foundations such as piled raft foundations but improvements are necessary in order to calculate realistic stress distributions along the pile.

Results from a case history where the designed foundation system for two adjacent towers consists of diaphragm wall panels with lengths between 20 - 30m have been presented. This foundation concept causes the smallest maximum and the differential displacements. The expected settlements of both towers is less than 80mm

With an alternative foundation system, namely piled raft foundation Layout 1, the maximum vertical displacement increases by roughly 50% and unfavourable differential settlements are computed. Piled raft foundation Layout 2 yields maximum vertical displacements in the region of tower I of 87mm and could be a feasible alternative, at least from a theoretical point of view.

6. REFERENCES

Arslan, U., Katzenbach, R., Quick, H., Gutwald, J. (1994) "Dreidimensionale Interaktionsberechnung zur Gründung der vier neuen Hochhaustürme in Frankfurt am Main", Proc. Deutsche Baugrundtagung 1994, Köln, Germany, pp. 425-437.

Benz, T. (2007) "Small-strain stiffness of soils and its numerical consequences", Dissertation. Mitteilung 55 des Instituts für Geotechnik. Universität Stuttgart.

Brinkgreve, R.B.J. & Swolfs, W.M. (2007) "Plaxis 3D Foundation. Finite element code for soil and rock analyses", Users manual, Netherlands.

Chow, Y.K. & Teh, C.I. (1991) "Pile-cap-pile-group interaction in nonhomogeneous soil", Journal of Geotechn. Engng, ASCE, Vol. 11, No 11, pp. 1655-1668.

Desai, C.S., Johnson L.D., Hargett C.M. (1974) "Analysis of pile supported gravity lock", Journal of Geotechn. Engng, ASCE, Vol. 100, GT 9, pp. 1009-1029.

Engin, H.K. (2006) "A report on embedded piles", Plaxis internal report.

Liu, W. & Novak, M. (1991) "Soil-pile-cap static interaction analysis by finite and infinite elements", Canadian Geotechnical Journal, Vol. 28, No. 6, pp. 771-783.

Martak, L., Mayerhofer, A.F., Tschuchnigg, F., Vorwagner, A. (2007) "Bahnhof Wien Mitte – Ein zentrales Infrastrukturprojekt im Herzen Wiens". In M. Dietzel et al. (eds.), Proc. 23th Christian Veder Kolloquium, Graz, pp. 79-96.

Prakoso, W.A.; Kulhawy, F.H. (2001) "Contribution to piled raft design", Journal of Geotechnical and Geoenvironmental Engineering, ASCE, Vol. 127 (1), pp. 17-24.

Reul, O. (2004) "Numerical study of the bearing behavior of piled rafts", International Journal of Geomechanics, ASCE, Vol. 4, No.2, pp. 59-68.

Sadek, M. & Shahrour, I. (2004) "A three dimensional embedded beam element for reinforced geomaterials", Intern. J. f. Numerical and Analytical Methods in Geomechanics 28(9): pp. 931-946.

Schanz, T., Vermeer, P.A., Bonnier, P.G. (1999) "The Hardening-Soil Model: Formulation and Verification". In R.B.J. Brinkgreve (ed.), Beyond 2000 in Computational Geotechnics: pp. 281-290.

Tschuchnigg, F. & Schweiger, H.F. (2008) "Comparison of different models for analysing foundations on jet grout columns", Proceedings of 12th Intern. Conf. of IACMAG, Goa, pp. 3149-3157.

Tschuchnigg, F. & Schweiger, H.F. (2009) "Numerical study of simplified piled raft foundations employing an embedded pile formulation". In S.Pietruszczak et al. (eds.), Conference of Computational Geomechanics; Proc. intern. Conf., Juan-les-Pins, 29 April-1 May 2009: pp. 743-752.

Tschuchnigg, F. & Schweiger, H.F. (2010) "Study of a complex deep foundation system using 3D finite element analysis". In T. Benz & S. Nordal (eds.), Conference of numerical methods in geotechnical engineering; Proc. Intern. Conf., Trondheim, 2-4 June 2010: pp. 679-684.

Tschuchnigg, F. & Schweiger, H.F. (2011) "Comparison of deep foundation systems using 3D Finite Element analysis", Proc. 13th Intern. Conf. Computer Methods and Advances in Geomechanics, (Khalili & Oeser, eds.), Sydney, Australia 2011, pp. 970-975.

Wehnert, M., Benz, T., Gollub, B., Cubaleski, T. (2010) "Settlement analysis of a large piled raft foundation", Proc. Numerical methods in geotechnical engineering NUMGE 2010, Benz & Nordal (eds.), Trondheim, Norway, pp. 673-678.